

# Polarized deeply inelastic scattering (DIS) structure functions for nucleons and nuclei

Ali N. Khorramian,<sup>1,2,\*</sup> S. Atashbar Tehrani,<sup>2,†</sup> S. Taheri Monfared,<sup>1,2,‡</sup> F. Arbabifar,<sup>1,§</sup> and F. I. Olness<sup>3,||</sup>

<sup>1</sup>*Physics Department, Semnan University, Semnan, Iran*

<sup>2</sup>*School of Particles and Accelerators, Institute for Research in Fundamental Sciences (IPM), P.O. Box 19395-5531, Tehran, Iran*

<sup>3</sup>*Department of Physics, Southern Methodist University, Dallas, Texas 75275-0175, USA*

(Received 29 November 2010; published 11 March 2011)

We extract parton distribution functions (PDFs) and structure functions from recent experimental data of polarized lepton–deeply inelastic scattering (DIS) on nucleons at next-to-leading order (NLO) quantum chromodynamics. We apply the Jacobi polynomial method to the Dokshitzer-Gribov-Lipatov-Altarelli-Parisi (DGLAP) evolution as this is numerically efficient. Having determined the polarized proton and neutron spin structure, we extend this analysis to describe <sup>3</sup>He and <sup>3</sup>H polarized structure functions, as well as various sum rules. We compare our results with other analyses from the literature.

DOI: 10.1103/PhysRevD.83.054017

PACS numbers: 13.60.Hb, 12.39.-x, 14.65.Bt

## I. INTRODUCTION

A fundamental challenge of high energy particle physics is to understand the spin structure of protons, neutrons, and nuclei in terms of their parton constituents. The increasing precision of experimental data on inclusive polarized deeply inelastic scattering (DIS) of leptons from nucleons allows us to perform incisive QCD analyses of polarized structure functions to reveal the spin-dependent partonic structure function of the nucleon. Polarized DIS lepton-nucleon scattering experiments have been performed at CERN, SLAC, DESY, and JLAB [1–13], and these processes have played a key role in our understanding of QCD and the spin structure of the nucleon [14–18]. There are several comprehensive analyses of the polarized DIS data in the literature [19–44]; this work provides a detailed picture of the spin structure of the nucleons.

The new precision experimental data from the HERMES and COMPASS Collaborations [12,13] of the spin structure function  $g_1$  provides additional information that we shall use to study the spin structure and quark helicity distributions. We shall choose an approach based on the expansion of orthogonal polynomials; specifically, we will implement Jacobi polynomials as we use experimental data for each bin of  $Q^2$  separately [43]. Previously [44], we applied the Jacobi polynomials to determine the polarized valon distributions using only the proton experimental data. In this analysis, both the unpolarized and polarized valon distributions were extracted, so more unknown parameters were required as compared to the present analysis. The Jacobi polynomial expansion has also been applied to a variety of QCD analyses [45–66], including the case of polarized parton distribution functions (PDFs) [44,67–73].

In the present study, we perform a NLO QCD analysis of the polarized deep inelastic data [3–13] in the  $\overline{\text{MS}}$  scheme and extract parametrizations of the polarized PDFs and structure functions. In Sec. II, we provide an overview of the Jacobi polynomials approach. In Sec. III we review the parametrization and evolution of the PDFs. In Sec. IV we present the results of our fit to the data, and in Sec. V we compute the associated structure functions and sum rules. Sec. VI contains the conclusions. We also provide an appendix which describes the FORTRAN code which is available.

## II. THE JACOBI POLYNOMIAL METHOD

We perform a NLO fit of the polarized parton distribution functions (PPDFs) using Jacobi polynomials to reconstruct the  $x$ -dependent quantities from their Mellin moments. The use of Jacobi polynomials has a number of advantages; specifically, it will allow us to factorize the  $x$  and  $Q^2$  dependence in a manner that allows an efficient parametrization and evolution of the structure functions.

For example, if we consider the spin structure function  $xg_1(x, Q^2)$ , we can expand this as

$$xg_1(x, Q^2) = x^\beta(1-x)^\alpha \sum_{n=0}^{N_{\max}} a_n(Q^2) \Theta_n^{\alpha, \beta}(x). \quad (1)$$

Here,  $\Theta_n^{\alpha, \beta}(x)$  are Jacobi polynomials of order  $n$ , and  $N_{\max}$  is the maximum order of our expansion. In this instance, the Jacobi polynomials allow us to factor out the essential part of the  $x$  dependence of the structure function into a weight function [45], and the  $Q^2$  dependence is contained in the Jacobi moments  $a_n(Q^2)$ .

To be more specific, the  $x$  dependence of the Jacobi polynomials can be written as

$$\Theta_n^{\alpha, \beta}(x) = \sum_{j=0}^n c_j^{(n)}(\alpha, \beta)x^j, \quad (2)$$

where the  $c_j^{(n)}(\alpha, \beta)$  coefficients are combinations of  $\Gamma$  functions involving  $\{n, \alpha, \beta\}$ . The Jacobi polynomials

\*Khorramiana@theory.ipm.ac.ir

†Atashbar@ipm.ir

‡Sara.taherimonfared@gmail.com

§Farbabifar@gmail.com

||olness@smu.edu

satisfy an orthogonality relation with weight function  $x^\beta(1-x)^\alpha$  as follows:

$$\int_0^1 dx x^\beta (1-x)^\alpha \Theta_k^{\alpha,\beta}(x) \Theta_l^{\alpha,\beta}(x) = \delta_{k,l}. \quad (3)$$

Thus, given the Jacobi moments  $a_n(Q^2)$ , the polarized structure function  $xg_1(x, Q^2)$  may be reconstructed from Eq. (1) [44].

We can compute the Jacobi moments  $a_n(Q^2)$  using the orthogonality relation to invert Eq. (1) to obtain

$$\begin{aligned} a_n(Q^2) &= \int_0^1 dx x g_1(x, Q^2) \Theta_k^{\alpha,\beta}(x) \\ &= \sum_{j=0}^n c_j^{(n)}(\alpha, \beta) \mathbf{M}[xg_1, j+2]. \end{aligned} \quad (4)$$

In Eq. (4), we have substituted Eq. (1) for  $xg_1(x, Q^2)$  and introduced the Mellin transform:

$$\mathbf{M}[xg_1, N] \equiv \int_0^1 dx x^{N-2} x g_1(x, Q^2). \quad (5)$$

We can now relate the polarized structure function  $xg_1(x, Q^2)$  with its moments [44]

$$\begin{aligned} xg_1(x, Q^2) &= x^\beta (1-x)^\alpha \sum_{n=0}^{N_{\max}} \Theta_n^{\alpha,\beta}(x) \\ &\times \sum_{j=0}^n c_j^{(n)}(\alpha, \beta) \mathbf{M}[xg_1, j+2]. \end{aligned} \quad (6)$$

Given Eq. (6) for  $xg_1(x, Q^2)$ , we choose the set  $\{N_{\max}, \alpha, \beta\}$  to achieve optimal convergence of this series throughout the kinematic region constrained by the data. In practice, we find  $N_{\max} = 9$ ,  $\alpha = 3.0$ , and  $\beta = 0.5$  to be sufficient.

### III. QCD ANALYSIS & PARAMTRIZATION

#### A. Parametrization

We consider a proton comprised of massless partons with helicity distributions  $q_\pm(x, Q^2)$  which carry momentum fraction  $x$  with a characteristic scale  $Q$ . The difference  $\delta q(x, Q^2) = q_+(x, Q^2) - q_-(x, Q^2)$  measures how much the parton of flavor  $q$  “remembers” of the parent proton polarization. We will parametrize these polarized PDFs at initial scale  $Q_0^2 = 4 \text{ GeV}^2$  using the following form:

$$x \delta q(x, Q_0^2) = \mathcal{N}_q \eta_q x^{a_q} (1-x)^{b_q} (1 + c_q x), \quad (7)$$

where the polarized PDFs are determined by parameters  $\{\eta_q, a_q, b_q, c_q\}$ , and the generic label  $q = \{u_v, d_v, \bar{q}, g\}$  denotes the partonic flavors up-valence, down-valence, sea, and gluon, respectively. The normalization constants  $\mathcal{N}_q$

$$\frac{1}{\mathcal{N}_q} = \left( 1 + c_q \frac{a_q}{a_q + b_q + 1} \right) B(a_q, b_q + 1), \quad (8)$$

are chosen such that  $\eta_i$  are the first moments of  $\delta q_i(x, Q_0^2)$ ,  $\eta_i = \int_0^1 dx \delta q_i(x, Q_0^2)$ , where  $B(a, b)$  is the Euler beta function.

The total up and down PDFs are a sum of the valence plus sea distributions:  $\delta u = \delta u_v + \delta \bar{q}$  and  $\delta d = \delta d_v + \delta \bar{d}$ . We will assume an  $SU(3)$  flavor symmetry such that  $\delta \bar{q} \equiv \delta \bar{u} = \delta \bar{d} = \delta s = \delta \bar{s}$ . While we could allow for an  $SU(3)$  symmetry violation term by introducing  $\kappa$  such that  $\delta s = \delta \bar{s} = \kappa \delta \bar{q}$ , as the strange PDF is poorly constrained the results would be insensitive to the specific choice of  $\kappa$ .

As seen from Eq. (7), each of four polarized parton densities  $q = \{u_v, d_v, \bar{q}, g\}$  contain four parameters  $\{\eta_q, a_q, b_q, c_q\}$  which gives a total of 16 parameters that we must constrain. We now demonstrate that we can eliminate some of these parameters while maintaining sufficient flexibility to obtain a good fit.

#### 1. First moments of $\delta u_v$ and $\delta d_v$

The parameters  $\eta_{u_v}$  and  $\eta_{d_v}$  are the first moments of the  $\delta u_v$  and  $\delta d_v$  polarized valence quark densities; these quantities can be related to  $F$  and  $D$  as measured in neutron and hyperon  $\beta$  decays according to the relations [74]:

$$a_3 = \int_0^1 dx \delta q_3 = \eta_{u_v} - \eta_{d_v} = F + D, \quad (9)$$

$$a_8 = \int_0^1 dx \delta q_8 = \eta_{u_v} + \eta_{d_v} = 3F - D, \quad (10)$$

where  $a_3$  and  $a_8$  are non-singlet combinations of the first moments of the polarized parton densities corresponding to

$$q_3 = (\delta u + \delta \bar{u}) - (\delta d + \delta \bar{d}), \quad (11)$$

$$q_8 = (\delta u + \delta \bar{u}) + (\delta d + \delta \bar{d}) - 2(\delta s + \delta \bar{s}). \quad (12)$$

A reanalysis of  $F$  and  $D$  with updated  $\beta$ -decay constants obtained [74]  $F = 0.464 \pm 0.008$  and  $D = 0.806 \pm 0.008$ . With these values we find

$$\eta_{u_v} = +0.928 \pm 0.014, \quad (13)$$

$$\eta_{d_v} = -0.342 \pm 0.018. \quad (14)$$

We make use of  $\eta_{u_v}$  and  $\eta_{d_v}$  to reduce the number of parameters by two.

#### 2. Gluon and Sea Quarks

We find the factor  $(1 + c_q x)$  in Eq. (7) provides flexibility to obtain a good description of the data, particularly for the valence distributions  $\{u_v, d_v\}$ . Thus, we will make use of the  $c_q$  coefficients for the up-valence and down-valence distributions; in contrast, we are able to set the values for  $c_{\bar{q}}$  and  $c_g$  to zero ( $c_{\bar{q}} = c_g = 0$ ) while maintaining a good fit and eliminating two free parameters. For the parameters  $\{c_{u_v}, c_{d_v}\}$  we find the fit improves if we use

TABLE I. Final parameter values and their statistical errors in the  $\overline{\text{MS}}$  scheme at the input scale  $Q_0^2 = 4 \text{ GeV}^2$ .

	$\eta_{u_v}$	0.928 (fixed)	$\eta_{\bar{q}}$	$-0.054 \pm 0.029$
$\delta u_v$	$a_{u_v}$	$0.535 \pm 0.022$	$\delta \bar{q}$	$0.474 \pm 0.121$
	$b_{u_v}$	$3.222 \pm 0.085$	$b_{\bar{q}}$	$9.310 \text{ (fixed)}$
	$c_{u_v}$	8.180 (fixed)	$c_{\bar{q}}$	0
$\delta d_v$	$\eta_{d_v}$	$-0.342 \text{ (fixed)}$	$\eta_g$	$0.224 \pm 0.118$
	$a_{d_v}$	$0.530 \pm 0.067$	$\delta g$	$2.833 \pm 0.528$
	$b_{d_v}$	$3.878 \pm 0.451$	$b_g$	$5.747 \text{ (fixed)}$
	$c_{d_v}$	4.789 (fixed)	$c_g$	0
	$\alpha_s(Q_0^2) = 0.381 \pm 0.017$			
	$\chi^2/\text{dof} = 273.6/370 = 0.74$			

nonzero values, but as these are relatively flat directions in  $\chi$ -space we shall fix the values as detailed in Table I.

Separately, we find the  $b$  parameters control the large- $x$  behavior of the PDFs; thus, the sea quark and gluon distributions have large uncertainties in this region as they are dominated by the valence. To provide some guidance, we observe that for *unpolarized* parton densities in the large- $x$  region, a ratio of  $b_{\bar{q}}/b_g \sim 1.6$  provides a good fit. Therefore, we impose this ratio on the *polarized*  $b_{\bar{q}}$  and  $b_g$  parameters to further reduce the free parameters. Additionally, we are able to extract reasonable constraints on the  $a_{\bar{q}}$  and  $a_g$  parameters; this is a benefit of the Jacobi polynomials.

Having fixed  $\{\eta_{u_v}, \eta_{d_v}, c_{\bar{q}}, c_g\}$  and the ratio  $b_{\bar{q}}/b_g$  in preliminary minimization, we then set the parameters  $\{b_{\bar{q}}, b_g, c_{u_v}, c_{d_v}\}$  as indicated in Table I; this gives us a total of 9 unknown parameters, in addition to  $\alpha_s(Q_0^2)$ .

## B. DGLAP evolution

In the Jacobi polynomial approach the Dokshitzer-Gribov-Lipatov-Altarelli-Parisi (DGLAP) evolution equations are solved in Mellin space. The Mellin transform of the parton densities  $q$  are defined analogous to that of Eq. (5):

$$\begin{aligned} \mathbf{M}[\delta q(x, Q_0^2), N] &\equiv \delta q(N, Q_0^2) = \int_0^1 x^{N-1} \delta q(x, Q_0^2) dx \\ &= \mathcal{N}_q \eta_q \left( 1 + c_q \frac{N-1+a_q}{N+a_q+b_q} \right) \\ &\quad \times (N-1+a_q, b_q+1), \end{aligned} \quad (15)$$

where  $q = \{u_v, d_v, \bar{q}, g\}$ , and  $B$  is the Euler beta function.

In Mellin space, the twist-2 contributions to the polarized structure function  $g_1(N, Q^2)$  can be represented in terms of the polarized parton densities and the coefficient functions  $\Delta C_i^N$  by

$$\begin{aligned} \mathbf{M}[g_1^p, N] &= \frac{1}{2} \sum_q e_q^2 \left[ \left( 1 + \frac{\alpha_s}{2\pi} \Delta C_q^N \right) [\delta q(N, Q^2) \right. \\ &\quad \left. + \delta \bar{q}(N, Q^2)] + \frac{\alpha_s}{2\pi} 2 \Delta C_g^N \delta g(N, Q^2) \right]. \end{aligned} \quad (16)$$

Here, the sum runs over quark flavors  $\{u, d, s\}$ , and  $\{\delta q, \delta \bar{q}, \delta g\}$  are the polarized quark, antiquark, and gluon distributions, respectively.

The coefficient functions  $\Delta C_i^N$  are the  $N$ th moments of spin-dependent Wilson coefficients, and are given by [16]

$$\begin{aligned} \Delta C_q^N &= \frac{4}{3} \left\{ -S_2(N) + (S_1(N))^2 + \left( \frac{3}{2} - \frac{1}{N(N+1)} \right) S_1(N) \right. \\ &\quad \left. + \frac{1}{N^2} + \frac{1}{2N} + \frac{1}{N+1} - \frac{9}{2} \right\}, \\ \Delta C_g^N &= \frac{1}{2} \left[ -\frac{N-1}{N(N+1)} (S_1(N)+1) - \frac{1}{N^2} + \frac{2}{N(N+1)} \right], \end{aligned}$$

with  $S_1(n) = \sum_{j=1}^n \frac{1}{j} = \psi(n+1) + \gamma_E$ ,  $S_2(n) = \sum_{j=1}^n \frac{1}{j^2} = (\frac{\pi^2}{6}) - \psi'(n+1)$ ,  $\psi(n) = \Gamma'(n)/\Gamma(n)$ , and  $\psi'(n) = d^2 \ln \Gamma(n)/dn^2$ .

In summary, we are able to express  $x g_1^p$  in terms of 9 unknown parameters at an input scale of  $Q_0^2 = 4 \text{ GeV}^2$ . We now examine the fits to the spin structure functions to extract the polarized PDFs from the available data.

## IV. QCD FIT OF $x g_1(x, Q^2)$ DATA

Our analysis is performed using the QCD-PEGASUS program [75]. We work at NLO in the QCD evolution using  $N_f = 3$  in the fixed-flavor number scheme with massless partonic flavors  $\{u, d, s\}$ . We take the renormalization and factorization scales to be equal ( $\mu_R = \mu_F$ ), and we compute the strong coupling  $\alpha_s(Q^2)$  at NLO using a fourth-order Runge-Kutta integration. Our initial parametrizations (Eq. (7)) are chosen to be invertible in N-space, and this makes our fitting procedure numerically efficient.

For the proton data we use EMC [3], HERMES [5,12], SMC [8], E143 [9], E155 [11] and COMPASS [13], for the neutron data we use E142 [4], HERMES [5,12], and E154 [6,7], and for the deuteron data we use SMC [8], E143 [9], E155 [10], and HERMES [12]. This data is summarized in Table II.

We minimize the global  $\chi^2$  [63,66,76],

$$\chi_{\text{global}}^2 = \sum_n w_n \chi_n^2, \quad (17)$$

where the sum  $n$  runs over the different experiments,  $w_n$  is a weight factor for the  $n$ th experiment, and  $\chi_n^2$  is given by

$$\chi_n^2 = \left( \frac{1 - \mathcal{N}_n}{\Delta \mathcal{N}_n} \right)^2 + \sum_i \left( \frac{\mathcal{N}_n g_{1,i}^{\text{exp}} - g_{1,i}^{\text{theor}}}{\mathcal{N}_n \Delta g_{1,i}^{\text{exp}}} \right)^2. \quad (18)$$

Here,  $g_{1,i}^{\text{exp}}$ ,  $\Delta g_{1,i}^{\text{exp}}$ , and  $g_{1,i}^{\text{theor}}$  denote the experimental measurement, the experimental uncertainty (statistical and systematic combined in quadrature) and theoretical value for the  $i$ th data point, respectively.  $\Delta \mathcal{N}_n$  is the experimental normalization uncertainty and  $\mathcal{N}_n$  is an overall normalization factor for the data of experiment  $n$ . We allow for a relative normalization shift  $\mathcal{N}_n$  between different

TABLE II. Published data points with the measured  $x$  and  $Q^2$  ranges, the number of data points (with a cut of  $Q^2 \geq 1.0 \text{ GeV}^2$ ), and the fitted normalization shifts  $\mathcal{N}_i$ .

Experiment	$x$ range	$Q^2$ range [ $\text{GeV}^2$ ]	# of data points	$\mathcal{N}_i$
E143 ( $p$ )	0.031–0.749	1.27–9.52	28	0.9998
HERMES ( $p$ )	0.028–0.66	1.01–7.36	39	1.0006
SMC ( $p$ )	0.005–0.480	1.30–58.0	12	0.9999
EMC ( $p$ )	0.015–0.466	3.50–29.5	10	1.0094
E155	0.015–0.750	1.22–34.72	24	1.0226
HERMES06 ( $p$ )	0.026–0.731	1.12–14.29	51	0.9992
COMPASS10 ( $p$ )	0.005–0.568	1.10–62.10	15	0.9920
<i>Proton</i>			179	
E143 ( $d$ )	0.031–0.749	1.27–9.52	28	0.9990
E155 ( $d$ )	0.015–0.750	1.22–34.79	24	0.9998
SMC ( $d$ )	0.005–0.479	1.30–54.80	12	0.9999
HERMES06 ( $d$ )	0.026–0.731	1.12–14.29	51	0.9976
<i>Deuteron</i>			115	
E142 ( $n$ )	0.035–0.466	1.10–5.50	8	0.9991
HERMES ( $n$ )	0.033–0.464	1.22–5.25	9	0.9999
E154 ( $n$ )	0.017–0.564	1.20–15.00	17	0.9996
HERMES06 ( $n$ )	0.026–0.731	1.12–14.29	51	1.0000
<i>Neutron</i>			85	
<i>Total</i>			379	

data sets within uncertainties  $\Delta \mathcal{N}_n$  quoted by the experiments.

We minimize the above  $\chi^2$  value with the 9 unknown parameters plus an undetermined  $\alpha_s(Q_0^2)$ . The values of these parameters are summarized in Table I. We find  $\chi^2/\text{d.o.f.} = 273.6/370$  which yields an acceptable fit to the experimental data.

## V. PDF AND STRUCTURE FUNCTION ANALYSIS

We next present our polarized PDFs and perform comparisons with other recent parametrizations [28,31–34].

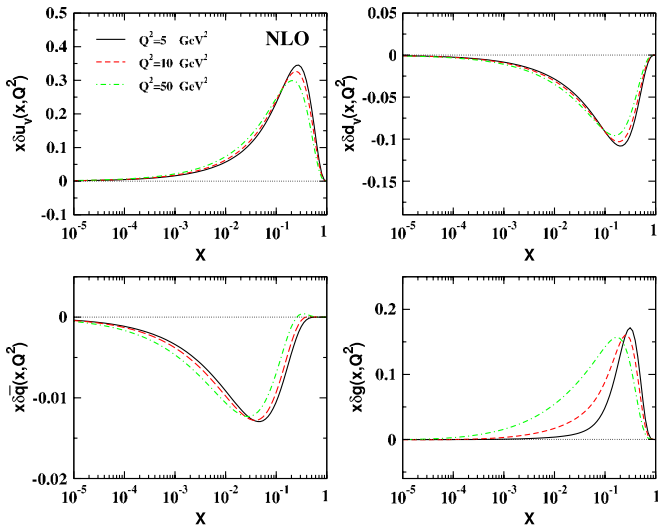


FIG. 1 (color online). The polarized parton distribution as function of  $x$  and for different values of  $Q^2$ .

## A. Polarized PDFs

Figure 1 displays our polarized PDFs for a selection of  $Q^2$  values. The up-valence ( $x\delta u_v$ ) and gluon ( $x\delta g$ ) distributions are positive, while the down-valence ( $x\delta d_v$ ) and sea ( $x\delta \bar{q}$ ) distributions are negative. We observe that the evolution shifts all the distributions to smaller values of  $x$ , and tends to flatten out the peak for increasing  $Q^2$ . Figure 2 displays the extracted NLO polarized PDFs as compared with various parametrizations from the literature [28,38–40].

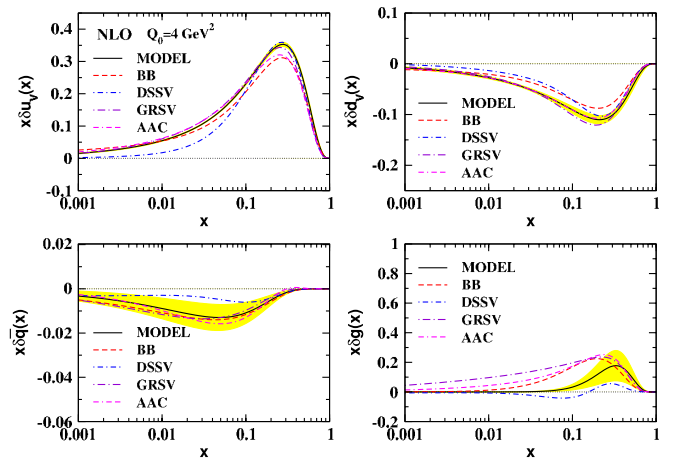


FIG. 2 (color online). The polarized parton distribution at  $Q_0^2 = 4 \text{ GeV}^2$  as a function of  $x$ . Our fit is the solid curve. Also shown are the results of BB (dashed) [40], DSSV (dashed-dotted) [38], GRSV (long dashed-dotted) [28], and AAC (dash-dashed-dotted) [39].

Examining the  $x\delta u_v$  and  $x\delta \bar{q}$  distributions we see that most of the fits are in agreement, with the possible exception of the de Florian–Sassot–Stratmann–Vogelsang (DSSV) [38] curves; for both distributions, the DSSV results approach zero more quickly than the other curves. For the  $x\delta d_v$  distribution, all of the curves are comparable. The DSSV analysis employs results from semi-inclusive DIS (SI-DIS) data which can impose individual constraints on individual quark flavor distributions in the nucleon [38]. Finally, for the gluon distribution, the DSSV results have a sign change in the region of  $x \sim 0.1$  while the other fits are positive. Our result for gluon distribution is located between the DSSV curve and the other fits [28,39,40]. In particular, we find the gluon polarization vanished more quickly for small  $x$  values as compared with the other fits; we conjecture that using available asymmetry data in the low  $x$  region may contribute to this difference.

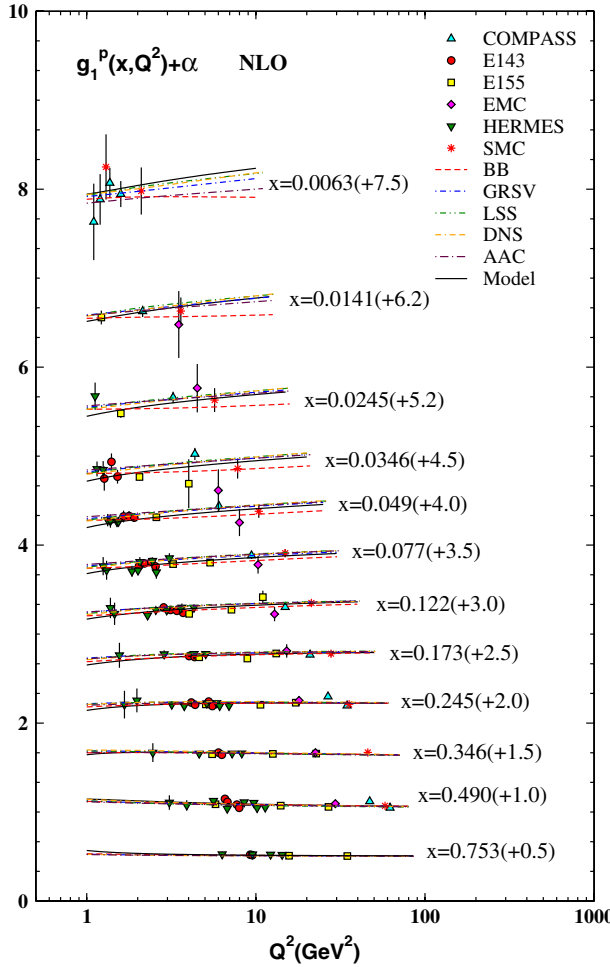


FIG. 3 (color online). The polarized structure function  $g_1^p$  as function of  $Q^2$  in intervals of  $x$ . The error bars shown are the statistical and systematic uncertainties added in quadrature. Our fit is the solid curve. The values of the shift  $\alpha$  are given in parentheses. Also shown are the results of BB [31], GRSV [28], LSS [34], DNS [33], and AAC [32].

## B. $g_1$ Structure functions

Figure 3 displays results for the polarized structure function  $xg_1^p$ . For comparison, we display the results obtained by Blumlein and Bottcher (BB) [31]; Gluck, Reya, Stratmann, and Vogelsang (GRSV) [28]; Leader, Sidorov, Stamenov (LSS) [34]; de Florian, Navarro, Sassot (DNS) [33]; and the Asymmetry Analysis Collaboration (AAC) [32]. There is some spread in the analyses at low values of  $x$ ; however, the data are generally well described within errors. As in the unpolarized case, the presence of scaling violations result a slope that varies with changing  $x$  values; this is evident in Fig. 3 where we observe the  $Q^2$  dependence of the structure function  $g_1(x, Q^2)$ .

Given the polarized proton PDFs, we can use isospin symmetry to obtain the corresponding neutron structure functions. In Fig. 4, we plot the neutron polarized structure function  $xg_1^n$ . We also display the NLO QCD curves obtained by Ref. [44] in the polarized valon model (PVM).

We can relate the deuteron structure function to that of the proton and neutron via

$$\mathbf{M}[g_1^d, N] = \frac{1}{2} \left( 1 - \frac{3}{2} \omega_D \right) (\mathbf{M}[g_1^p, N] + \mathbf{M}[g_1^n, N]), \quad (19)$$

where  $\omega_D = 0.05 \pm 0.01$  is the  $D$ -state wave probability for the deuteron [77]. In Fig. 5 we present our results for the structure functions  $xg_1^p(x, Q^2)$ ,  $xg_1^n(x, Q^2)$ , and  $xg_1^d(x, Q^2)$ , and this compares favorably with the results of the BB [31], GRSV [28], LSS [34], DNS [33], and AAC [32] analyses.

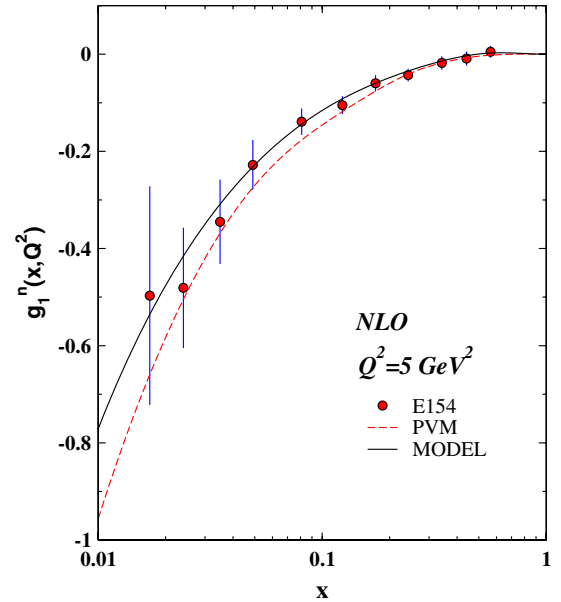


FIG. 4 (color online). The polarized structure function  $xg_1^n$  as function of  $x$  and for a fixed value of  $Q^2 = 5 \text{ GeV}^2$ . The present fit is the solid curve. Also shown are the results of AK [44] (dashed) according to polarized valon model (PVM).

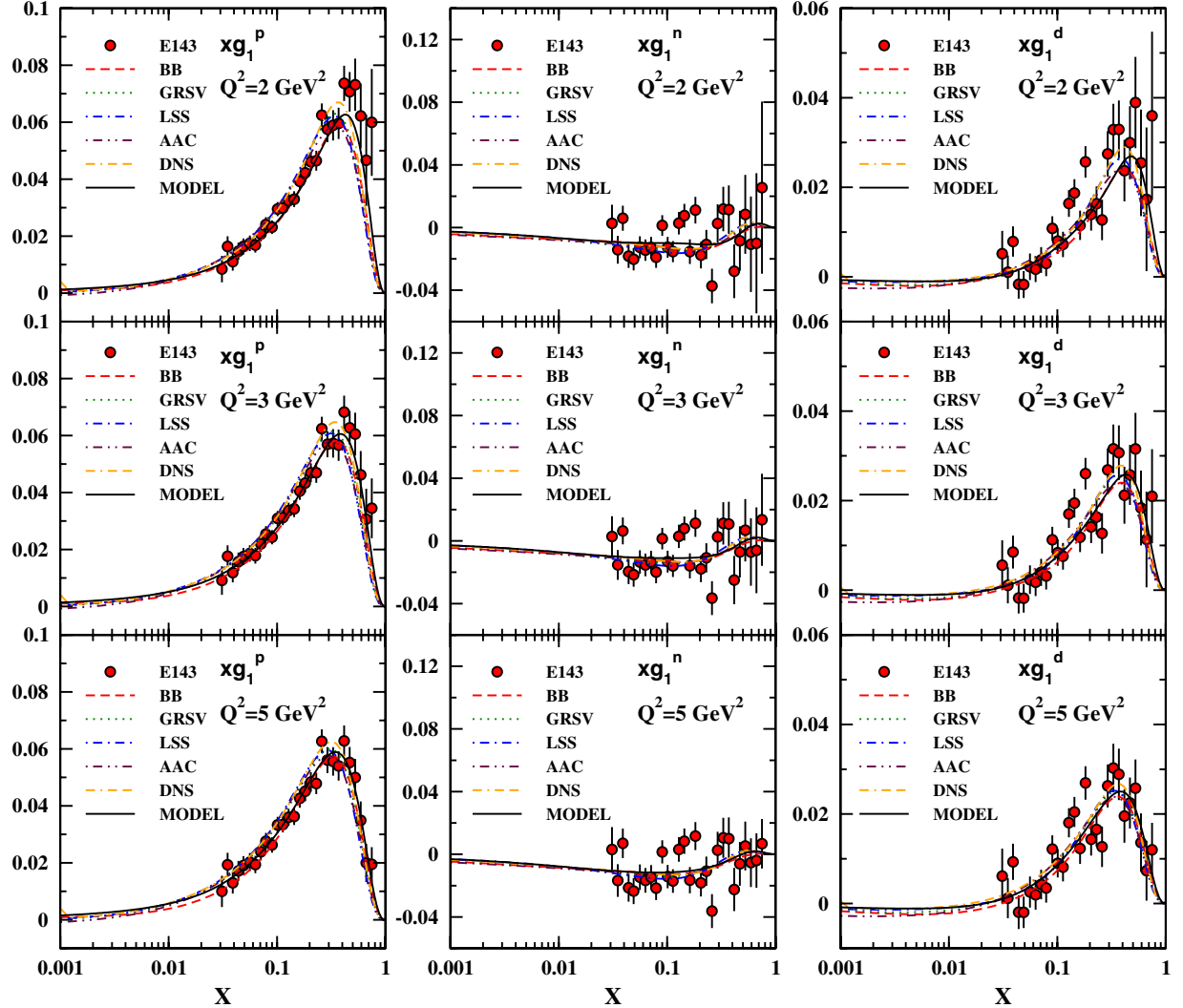


FIG. 5 (color online). The polarized structure function  $xg_1^P$ ,  $xg_1^n$  and  $xg_1^d$  as a function of  $x$  for selected values of  $Q^2$ . The data are well described by the fit (solid curve). Also shown are the QCD NLO curves obtained by BB (dashed) [31], GRSV (dotted) [28], LSS (dash-dotted) [34], AAC (dash-dot-dotted) [32], and DNS (dash-dash-dotted) [33].

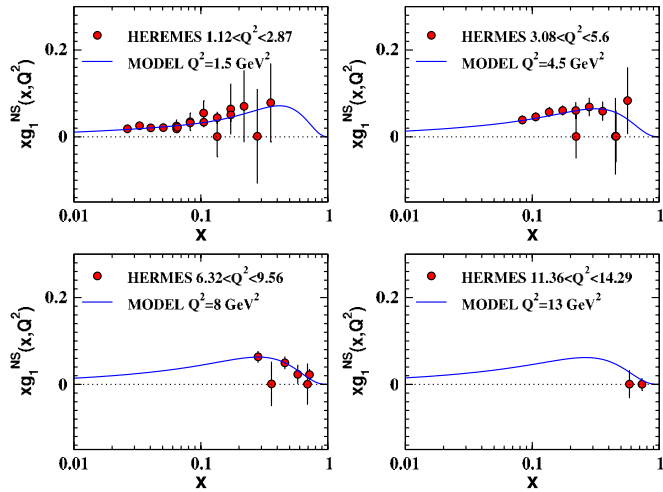


FIG. 6 (color online). The non-singlet polarized structure function  $xg_1^{NS}$  as function of  $x$ .

The non-singlet spin structure function  $xg_1^{NS}(x, Q^2)$  is defined as [12]

$$\begin{aligned} xg_1^{NS}(x, Q^2) &\equiv xg_1^P(x, Q^2) - xg_1^n(x, Q^2) \\ &= 2 \left[ xg_1^P(x, Q^2) - \frac{xg_1^d(x, Q^2)}{1 - \frac{3}{2}\omega_D} \right]. \end{aligned} \quad (20)$$

This is displayed in Fig. 6, and we compare with the HERMES data [12] for various  $Q^2$  bins. In the second line of Eq. (20) we have related the structure function of the deuteron using isospin symmetry and the relation of Eq. (19).

### C. $g_2$ Structure function

We can now extract the structure function  $xg_2$  via the Wandzura-Wilczek relation [78,79]:

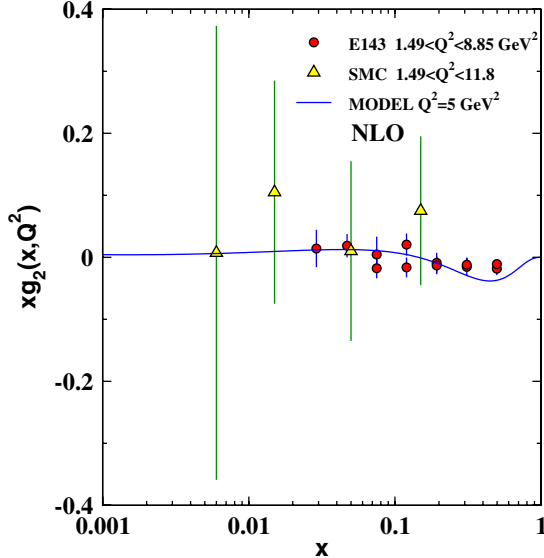


FIG. 7 (color online). The polarized structure function  $xg_2$  as function of  $x$  for  $Q^2 = 5 \text{ GeV}^2$ .

$$g_2(x, Q^2) = -g_1^p(x, Q^2) + \int_x^1 \frac{dy}{y} g_1^p(y, Q^2). \quad (21)$$

This relation remains valid in the presence of target mass corrections. In Fig. 7 we show our result for  $xg_2$  and we compare it with the experimental data from E143 [9] and SMC [8].

#### D. First moment of $g_1$ structure functions

We next use the polarized PDFs to compute the first moments, and compare with other recent analyses. We can obtain the first moment of  $g_1^p$  by

$$\Gamma_1^p(Q^2) \equiv \int_0^1 dx g_1^p(x, Q^2). \quad (22)$$

The results of our fit are presented in Table III for selected values of  $Q^2$ , and these are compared with results from the literature in Table IV.

In the framework of QCD the spin of the proton can be expressed in terms of the first moment of the total quark

TABLE III. The first moments of polarized parton distributions,  $\Delta u_v$ ,  $\Delta d_v$ ,  $\Delta \bar{q}$ ,  $\Delta g$  and polarized structure functions  $\Gamma_1^p$ ,  $\Gamma_1^n$ ,  $\Gamma_1^d$  in NLO in the  $\overline{\text{MS}}$  scheme for some different values of  $Q^2$ .

$Q^2$	2 $\text{GeV}^2$	3 $\text{GeV}^2$	5 $\text{GeV}^2$	10 $\text{GeV}^2$
$\Delta u_v$	0.928 864	0.928 310	0.927 794	0.927 288
$\Delta d_v$	-0.342 318	-0.342 114	-0.341 924	-0.341 738
$\Delta \bar{q}$	-0.053 400	-0.053 893	-0.054 379	-0.054 789
$\Delta g$	0.143 610	0.191 313	0.248 845	0.323 886
$\Gamma_1^p$	0.128 291	0.131 199	0.133 822	0.136 303
$\Gamma_1^n$	-0.050 972	-0.052 416	-0.053 735	-0.055 000
$\Gamma_1^d$	0.035 296	0.035 965	0.036 559	0.037 115

TABLE IV. Comparison of the first moments of the polarized parton densities in NLO in the  $\overline{\text{MS}}$  scheme at  $Q^2 = 4 \text{ GeV}^2$  for different sets of recent parton parametrizations. The second column (“Model”) contains the first moments which are obtained from our new parametrization based on the Jacobi polynomials expansion method. The BB [40], GRSV [28], and AAC [32] results are also shown.

Model	BB [40]	GRSV [28]	AAC [32]
$\Delta u_v$	0.928	0.928	0.9206
$\Delta d_v$	-0.342	-0.342	-0.3409
$\Delta u$	0.874	0.866	0.8593
$\Delta d$	-0.396	-0.404	-0.4043
$\Delta \bar{q}$	-0.054	-0.062	-0.0625
$\Delta g$	0.224	0.462	0.6828

and gluon helicity distributions and their orbital angular momentum, i.e.,

$$\frac{1}{2} = \frac{1}{2} \Delta \Sigma^p + \Delta g^p + L_z^p, \quad (23)$$

where  $L_z^p$  is the total orbital angular momentum of all quarks and gluons. The contribution of  $\frac{1}{2} \Delta \Sigma + \Delta g$  for typical value of  $Q^2 = 4 \text{ GeV}^2$  is around 0.355 in our analysis. We can also compare this value in NLO with other recent analysis. The reported value from the BB model [40] is 0.569, the AAC model [32] is 0.837, and the GRSV model [28] is 0.785, while the DSSV model [38] is approximately 0.1. Since the values of  $\frac{1}{2} \Delta \Sigma$  are comparable, we observe that the difference between the above reported values must come from different gluon distributions.

#### E. Strong coupling constant

In this QCD analysis we extract  $\alpha_s(Q_0^2)$  at NLO and obtain

$$\alpha_s(Q_0^2) = 0.381 \pm 0.017. \quad (24)$$

Rescaling this to the  $Z$  boson mass scale we find

$$\alpha_s(M_Z^2) = 0.1149 \pm 0.0015. \quad (25)$$

The error given in the above equation does not include the relative systematics of the different classes of measurements. In Table V we provide a comparison of this value with other determinations from the literature computed at NLO and higher orders, including the current world average of  $\alpha_s(M_Z^2) = 0.1184 \pm 0.0007$ .

#### F. Nuclear polarized structure functions

Using the polarized PDF fit results, we examine the nucleon corrections factors for  ${}^3\text{He}$  and  ${}^3\text{H}$ . The polarized structure functions  $g_1^p$  and  $g_1^n$  can be composed from the polarized proton structure  $g_1^p$  and the polarized neutron structure  $g_1^n$  as follows:

TABLE V. Comparison of  $\alpha_s(M_Z^2)$  values from the literature.

$\alpha_s(M_Z^2)$	Order	Reference	Notes
$0.1149 \pm 0.0015$	NLO	...	This analysis
$0.1132^{+0.0056}_{-0.0095}$	NLO	[40]	...
$0.1134^{+0.0019}_{-0.0021}$	NNLO	[80]	...
$0.1141 \pm 0.0036$	NLO	[44]	...
$0.1131 \pm 0.0019$	NNLO	[63]	...
$0.1139 \pm 0.0020$	NNNLO	[66]	...
$0.1141^{+0.0020}_{-0.0022}$	NNNLO	[80]	...
$0.1135 \pm 0.0014$	NNLO	[81]	FFS
$0.1129 \pm 0.0014$	NNLO	[81]	BSMN
$0.1124 \pm 0.0020$	NNLO	[82]	dynamic approach
$0.1158 \pm 0.0035$	NNLO	[82]	standard approach
$0.1171 \pm 0.0014$	NNLO	[83]	...
$0.1147 \pm 0.0012$	NNLO	[84]	...
$0.1145 \pm 0.0042$	NNLO	[85]	(Preliminary)
$0.1184 \pm 0.0007$	...	[86]	World Average

$$g_1^{^3\text{He}}(x, Q^2) = \int_x^3 \frac{dy}{y} \Delta f_{^3\text{He}}^n(y) g_1^n\left(\frac{x}{y}, Q^2\right) + 2 \int_x^3 \frac{dy}{y} \Delta f_{^3\text{He}}^p(y) g_1^p\left(\frac{x}{y}, Q^2\right) - 0.014[g_1^p(x, Q^2) - 4g_1^n(x, Q^2)], \quad (26)$$

$$g_1^{^3\text{H}}(x, Q^2) = 2 \int_x^3 \frac{dy}{y} \Delta f_{^3\text{H}}^n(y) g_1^n\left(\frac{x}{y}, Q^2\right) + \int_x^3 \frac{dy}{y} \Delta f_{^3\text{H}}^p(y) g_1^p\left(\frac{x}{y}, Q^2\right) + 0.014[g_1^p(x, Q^2) - 4g_1^n(x, Q^2)]. \quad (27)$$

Here,  $\Delta f_{^3\text{He}}^N(y)$  and  $\Delta f_{^3\text{H}}^N(y)$  are the spin-dependent nucleon light-cone momentum distributions [87,88]. These functions parametrize the Fermi motion and the nucleon binding, and are readily calculated using the ground-state wave functions of  ${}^3\text{He}$  and  ${}^3\text{H}$ . Note that the last term in above equations is important only in the large- $x$  region.

If we utilize isospin symmetry, we can equate  $\Delta f_{^3\text{He}}^p(y)$  to  $\Delta f_{^3\text{H}}^n(y)$ , and also  $\Delta f_{^3\text{He}}^n(y)$  to  $\Delta f_{^3\text{H}}^p(y)$ ; thus, we are left with only two independent functions  $\Delta f_{^3\text{He}}^p(y)$  and  $\Delta f_{^3\text{He}}^n(y)$ . Using the results of Refs. [88–90], we express these distributions as

$$\Delta f_{^3\text{He}}^n(y) = \frac{a^n e^{-(0.5(1-d^n)(-b^n+y)^2/(c^n)^2)}}{1 + \frac{d^n(-b^n+y)^2}{(c^n)^2}}, \quad (28)$$

$$\Delta f_{^3\text{He}}^p(y) = \frac{\sum_{i=0}^4 a_i^p U_i(y)}{\sum_{i=0}^4 b_i^p U_i(y)}, \quad (29)$$

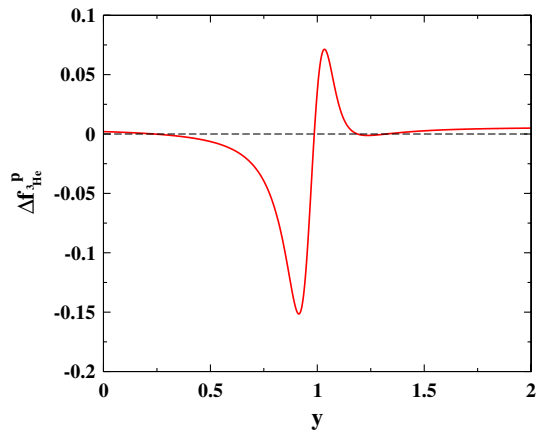
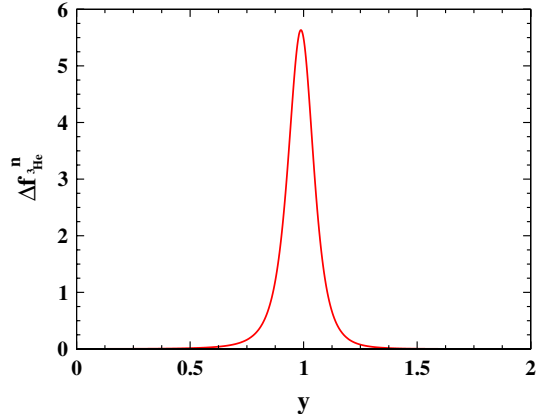
where  $U_n(y)$  is a Chebyshev polynomial of the second type. The numerical coefficients of these equations are

TABLE VI. Numerical coefficients for Eqs. (28) and (29), of  $\Delta f_{^3\text{He}}^n(y)$  and  $\Delta f_{^3\text{He}}^p(y)$  obtained from Refs. [88–90].

$n$	$p$	$p$
$a^n = 5.650556817$	$a_0^p = 0.0148376$	$b_0^p = 4.15388$
$b^n = 0.986818274$	$a_1^p = -0.0189575$	$b_1^p = -4.75525$
$c^n = 0.064446823$	$a_2^p = 0.0121792$	$b_2^p = 2.68417$
$d^n = 0.807650292$	$a_3^p = -0.0040397$	$b_3^p = -0.800306$
	$a_4^p = 0.000540845$	$b_4^p = 0.101095$

presented in Table VI. We can then use Eqs. (26) and (27) to obtain the polarized nucleon structure functions  $g_1^{^3\text{He}}(x, Q^2)$  and  $g_1^{^3\text{H}}(x, Q^2)$ .

To determine the  $g_1^{^3\text{He}}$  and  $g_1^{^3\text{H}}$  polarized structure functions we need the polarized light-cone distribution functions for proton and neutron in  ${}^3\text{He}$ , i.e.,  $\Delta f_{^3\text{He}}^p$  and  $\Delta f_{^3\text{He}}^n$ . In Figs. 8 and 9 we present our results using the parametrization of Eqs. (28) and (29), which is based on the numerical results of Ref. [90].

FIG. 8 (color online). The polarized light-cone distribution function for the proton in the  ${}^3\text{He}$ , based on the results of Ref. [88–90].FIG. 9 (color online). The polarized light-cone distribution function for the neutron in the  ${}^3\text{He}$ , based on the results of Ref. [88–90].

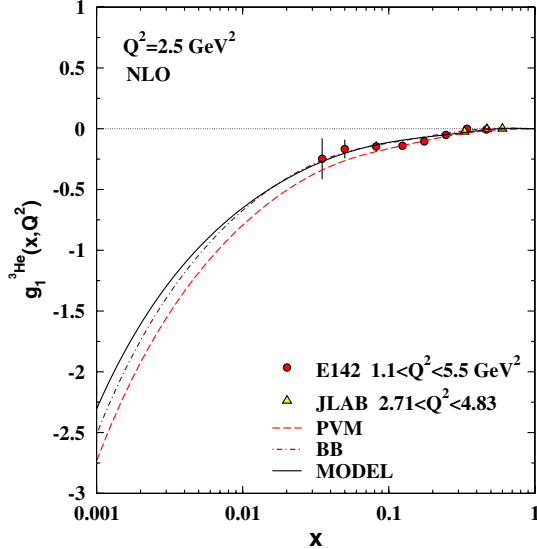


FIG. 10 (color online). Analytical result for the polarized  ${}^3\text{He}$  structure function v.s.  $x$  for fixed  $Q^2 = 2.5 \text{ GeV}^2$ . The current fit is the solid curve. Also shown are the QCD NLO curves obtained by AK (dashed) [44] according to polarized valon model (PVM) and BB (dashed-dotted) [31].

In Figs. 10 and 11 we show our results for the  $g_1^{^3\text{He}}$  and  $g_1^{^3\text{H}}$  polarized structure function, and compare with BB [31], and the PVM [44]. For the  $g_1^{^3\text{He}}$  polarized structure function we see that our result coincides with the BB fit for  $x$  values down to  $\sim 10^{-2}$ , and then falls off more quickly at very small  $x$  values. The polarized valon model (PVM), while still a reasonable fit to the data, lies below both of the other fits. For the  $g_1^{^3\text{H}}$  polarized structure function, our fit

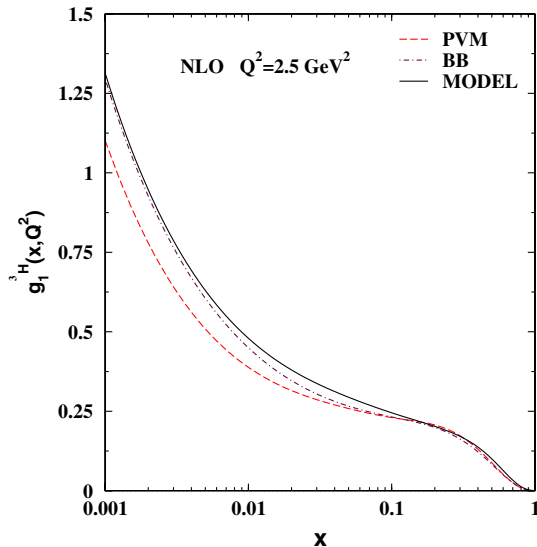


FIG. 11 (color online). Analytical result for the polarized  ${}^3\text{H}$  structure function v.s.  $x$  for fixed  $Q^2 = 2.5 \text{ GeV}^2$ . The current fit is the solid curve. Also shown are the QCD NLO curves obtained by AK (dashed) [44] according to polarized valon model (PVM) and BB (dashed-dotted) [31] for comparison.

coincides with the BB fit at both large and small  $x$  values, but dips below it (closer to the PVM) for intermediate  $x$  values. The differences between these curves come from the various data sets used, the constraints imposed, and the form of the parametrization. For example, in the AK fit [44], only 257 experimental data points were used as the neutron data were not included; in contrast, the present analysis uses 379 points which does include the neutron data. Furthermore, the AK fit used 15 free parameters while there are only 9 free parameters in the present analysis. These differences are reflected in the extractions of PPDFs, and a comparison of these different analyses may be indicative of the stability of the determined QCD parameters.

### G. Bjorken sum rule

We can also study the Bjorken sum rule [91] which relates the difference of the first moments of the proton and neutron spin structure functions to the axial vector coupling constant of the neutron  $\beta$ -decay,

$$\int_0^1 [g_1^p(x, Q^2) - g_1^n(x, Q^2)] dx = \frac{1}{6} g_A \left[ 1 + O\left(\frac{\alpha_s}{\pi}\right) \right], \quad (30)$$

where  $g_A = 1.2670 \pm 0.0035$  [74], and the QCD radiative corrections are denoted as  $O\left(\frac{\alpha_s}{\pi}\right)$ . This sum rule can be generalized for the  ${}^3\text{He}-{}^3\text{H}$  system as follows:

$$\int_0^1 [g_1^{^3\text{H}}(x, Q^2) - g_1^{^3\text{He}}(x, Q^2)] dx = \frac{1}{6} \tilde{g}_A \left[ 1 + O\left(\frac{\alpha_s}{\pi}\right) \right], \quad (31)$$

where  $\tilde{g}_A$  is the axial vector coupling constant of the Triton  $\beta$  decay, with  $\tilde{g}_A = 1.211 \pm 0.002$  [92]. Taking the ratio of the Eqs. (30) and (31), we find

$$\frac{\int_0^1 [g_1^{^3\text{H}}(x, Q^2) - g_1^{^3\text{He}}(x, Q^2)] dx}{\int_0^1 [g_1^p(x, Q^2) - g_1^n(x, Q^2)] dx} = \frac{\tilde{g}_A}{g_A}. \quad (32)$$

Given  $g_A$  and  $\tilde{g}_A$ , we compute the above ratio to be 0.956 [88]. Note that the QCD radiative corrections are expected to cancel exactly in above equation. Using the Bjorken sum rules of Eqs. (30) and (31), we obtain the value 0.924 for the ratio of Eq. (32).

## VI. CONCLUSIONS

We have presented a fit to the polarized lepton-DIS data on nuclei at NLO QCD using the Jacobi polynomial method. Having extracted the polarized PDFs, we compute various nuclear structure functions ( $g_1, g_2$ ) and Bjorken sum rule. In general, we find good agreement with the experimental data, and our results are in accord with other determinations from the literature; collectively, this demonstrates progress of the field toward a detailed description of the spin structure of the nucleon.

Having demonstrated the compatibility of the Jacobi polynomial method with other approaches in the literature,

this study can serve as a foundation for addressing issues of polarized scattering processes from a complementary perspective. In particular, the Jacobi polynomial method offers the opportunity to examine efficiencies of different methods, and this work is in progress.

## ACKNOWLEDGMENTS

We thank S. Kumano and M. Miyama of the ACC Collaboration for allowing us to use their interpolation routines. A. N. K. thanks Johannes Blümlein for useful discussions, and is grateful to A. L. Kataev for the suggestion of the Jacobi polynomial method, the CERN TH-PH division for the hospitality where a portion of this work was performed, and Semnan University for financial support. We acknowledge financial support of the School of Particles and Accelerators, Institute for Research in Fundamental

Sciences (IPM). This work was partially supported by the U.S. Department of Energy under Grant No. DE-FG02-04ER41299, and the Lightner-Sams Foundation.

## APPENDIX: FORTRAN CODE

A FORTRAN package containing our  $g_1(x, Q^2)$  polarized structure functions for  $\{p, n, d, NS, {}^3\text{He}, {}^3\text{H}\}$  and  $xg_2^p(x, Q^2)$ , as well as the polarized parton densities  $\{u_v, d_v, g, \bar{q}\}$ ,  $x\delta u_v(x, Q^2)$ ,  $x\delta d_v(x, Q^2)$ ,  $x\delta g(x, Q^2)$ , and  $x\delta \bar{q}(x, Q^2)$  at NLO in the  $\overline{\text{MS}}$  scheme, can be found at <http://particles.ipm.ir/links/QCD.htm> or obtained via email from the authors. These functions are interpolated using cubic splines in  $Q^2$  and a linear interpolation in  $\log(Q^2)$ . The package includes an example program to illustrate the use of the routines.

- 
- [1] X. Zheng *et al.* (The JLAB Hall A Collaboration), *Phys. Rev. C* **70**, 065207 (2004).
  - [2] K. V. Dharmawardane *et al.* (CLAS Collaboration), *Phys. Lett. B* **641**, 11 (2006).
  - [3] J. Ashman *et al.* (European Muon Collaboration), *Phys. Lett. B* **206**, 364 (1988); *Nucl. Phys.* **B328**, 1 (1989).
  - [4] P. L. Anthony *et al.* (E142 Collaboration), *Phys. Rev. D* **54**, 6620 (1996).
  - [5] K. Ackerstaff *et al.* (HERMES Collaboration), *Phys. Lett. B* **404**, 383 (1997); A. Airapetian *et al.* (HERMES Collaboration), *Phys. Lett. B* **442**, 484 (1998).
  - [6] K. Abe *et al.* (E154 Collaboration), *Phys. Lett. B* **405**, 180 (1997).
  - [7] K. Abe *et al.* (E154 Collaboration), *Phys. Rev. Lett.* **79**, 26 (1997).
  - [8] B. Adeva *et al.* (Spin Muon Collaboration), *Phys. Rev. D* **58**, 112001 (1998).
  - [9] K. Abe *et al.* (E143 Collaboration), *Phys. Rev. D* **58**, 112003 (1998).
  - [10] P. L. Anthony *et al.* (E155 Collaboration), *Phys. Lett. B* **463**, 339 (1999).
  - [11] P. L. Anthony *et al.* (E155 Collaboration), *Phys. Lett. B* **493**, 19 (2000).
  - [12] A. Airapetian *et al.* (HERMES Collaboration), *Phys. Rev. D* **75**, 012007 (2007).
  - [13] M. G. Alekseev *et al.* (COMPASS Collaboration), *Phys. Lett. B* **690**, 466 (2010); V. Y. Alexakhin *et al.* (COMPASS Collaboration), *Phys. Lett. B* **647**, 8 (2007).
  - [14] G. Altarelli, [arXiv:0907.1751](https://arxiv.org/abs/0907.1751).
  - [15] M. Anselmino, A. Efremov, and E. Leader, *Phys. Rep.* **261**, 1 (1995); **281**, 399 (1997).
  - [16] B. Lampe and E. Reya, *Phys. Rep.* **332**, 1 (2000).
  - [17] E. W. Hughes and R. Voss, *Annu. Rev. Nucl. Part. Sci.* **49**, 303 (1999).
  - [18] B. W. Filippone and X. D. Ji, *Adv. Nucl. Phys.* **26**, 1 (2002).
  - [19] G. Altarelli, R. D. Ball, S. Forte, and G. Ridolfi, *Acta Phys. Pol. B* **29**, 1145 (1998).
  - [20] R. D. Ball, G. Ridolfi, G. Altarelli, and S. Forte, [arXiv: hep-ph/9707276](https://arxiv.org/abs/hep-ph/9707276).
  - [21] C. Bourrely, F. Buccella, O. Pisanti, P. Santorelli, and J. Soffer, *Prog. Theor. Phys.* **99**, 1017 (1998).
  - [22] D. de Florian, O. A. Sampayo, and R. Sassot, *Phys. Rev. D* **57**, 5803 (1998).
  - [23] L. E. Gordon, M. Goshtasbpour, and G. P. Ramsey, *Phys. Rev. D* **58**, 094017 (1998).
  - [24] E. Leader, A. V. Sidorov, and D. B. Stamenov, *Phys. Lett. B* **462**, 189 (1999); **445**, 232 (1998); *Phys. Rev. D* **58**, 114028 (1998); *Int. J. Mod. Phys. A* **13**, 5573 (1998).
  - [25] M. Stratmann, *Nucl. Phys. B, Proc. Suppl.* **79**, 538 (1999).
  - [26] D. K. Ghosh, S. Gupta, and D. Indumathi, *Phys. Rev. D* **62**, 094012 (2000).
  - [27] D. de Florian and R. Sassot, *Phys. Rev. D* **62**, 094025 (2000).
  - [28] M. Gluck, E. Reya, M. Stratmann, and W. Vogelsang, *Phys. Rev. D* **63**, 094005 (2001).
  - [29] R. S. Bhalerao, *Phys. Rev. C* **63**, 025208 (2001).
  - [30] E. Leader, A. V. Sidorov, and D. B. Stamenov, *Eur. Phys. J. C* **23**, 479 (2002).
  - [31] J. Blumlein and H. Bottcher, *Nucl. Phys. B* **636**, 225 (2002).
  - [32] Y. Goto *et al.* (Asymmetry Analysis Collaboration), *Phys. Rev. D* **62**, 034017 (2000); M. Hirai, S. Kumano, and N. Saito (Asymmetry Analysis Collaboration), *Phys. Rev. D* **69**, 054021 (2004).
  - [33] D. de Florian, G. A. Navarro, and R. Sassot, *Phys. Rev. D* **71**, 094018 (2005).
  - [34] E. Leader, A. V. Sidorov, and D. B. Stamenov, *Phys. Rev. D* **73**, 034023 (2006).
  - [35] C. Bourrely, J. Soffer, and F. Buccella, *Eur. Phys. J. C* **23**, 487 (2002).
  - [36] G. Altarelli *et al.*, *Nucl. Phys. B* **496**, 337 (1997); *Acta Phys. Pol. B* **29**, 1145 (1998); S. Forte, M. Mangano, and G. Ridolfi, *Nucl. Phys. B* **602**, 585 (2001).

- [37] G. Altarelli, R. D. Ball, S. Forte, and G. Ridolfi, *Nucl. Phys.* **B496**, 337 (1997).
- [38] D. de Florian, R. Sassot, M. Stratmann, and W. Vogelsang, *Phys. Rev. Lett.* **101**, 072001 (2008).
- [39] M. Hirai and S. Kumano (Asymmetry Analysis Collaboration), *Nucl. Phys.* **B813**, 106 (2009).
- [40] J. Blümlein and H. Bottcher, arXiv:1005.3113.
- [41] E. Leader, A. V. Sidorov, and D. B. Stamenov, arXiv:1007.4781.
- [42] J. Blümlein and H. Böttcher, *Nucl. Phys.* **B841**, 205 (2010).
- [43] A. N. Khorramian, A. Mirjalili, and S. A. Tehrani, *J. High Energy Phys.* **10** (2004) 062.
- [44] S. Atashbar Tehrani and A. N. Khorramian, *J. High Energy Phys.* **07** (2007) 048.
- [45] G. Parisi and N. Sourlas, *Nucl. Phys.* **B151**, 421 (1979); I. S. Barker, C. B. Langensiepen, and G. Shaw, *Nucl. Phys.* **B186**, 61 (1981).
- [46] I. S. Barker, B. R. Martin, and G. Shaw, *Z. Phys. C* **19**, 147 (1983); I. S. Barker and B. R. Martin, *Z. Phys. C* **24**, 255 (1984); S. P. Kurlovich, A. V. Sidorov, and N. B. Skachkov, JINR Report E2-89-655, Dubna, 1989.
- [47] V. G. Krivokhizhin, S. P. Kurlovich, V. V. Sanadze, I. A. Savin, A. V. Sidorov, and N. B. Skachkov, *Z. Phys. C* **36**, 51 (1987).
- [48] V. G. Krivokhizhin *et al.*, *Z. Phys. C* **48**, 347 (1990).
- [49] J. Chyla and J. Rames, *Z. Phys. C* **31**, 151 (1986).
- [50] I. S. Barker, C. S. Langensiepen, and G. Shaw, *Nucl. Phys.* **B186**, 61 (1981).
- [51] A. L. Kataev, A. V. Kotikov, G. Parente, and A. V. Sidorov, *Phys. Lett. B* **417**, 374 (1998).
- [52] A. L. Kataev, G. Parente, and A. V. Sidorov, arXiv:hep-ph/9809500.
- [53] A. L. Kataev, G. Parente, and A. V. Sidorov, *Nucl. Phys.* **B573**, 405 (2000).
- [54] A. L. Kataev, G. Parente, and A. V. Sidorov, *Phys. Part. Nucl.* **34**, 20 (2003); *Nucl. Phys. B, Proc. Suppl.* **116**, 105 (2003).
- [55] A. N. Khorramian, S. Atashbar Tehrani, and M. Ghominejad, *Acta Phys. Pol. B* **38**, 3551 (2007).
- [56] A. N. Khorramian and S. A. Tehrani, *J. Phys. Conf. Ser.* **110**, 022022 (2008).
- [57] A. N. Khorramian and S. A. Tehrani, *AIP Conf. Proc.* **1006**, 118 (2008).
- [58] S. Atashbar Tehrani and A. N. Khorramian, *Nucl. Phys. B, Proc. Suppl.* **186**, 58 (2009).
- [59] A. N. Khorramian, S. Atashbar Tehrani, H. Khanpour, and S. Taheri Monfared, *Hyperfine Interact.* **194**, 337 (2009).
- [60] A. N. Khorramian, S. Atashbar Tehrani, M. Soleymaninia, and S. Batebi, *Hyperfine Interact.* **194**, 341 (2009).
- [61] S. Atashbar Tehrani and A. N. Khorramian, *Hyperfine Interact.* **194**, 331 (2009).
- [62] S. Atashbar Tehrani and A. N. Khorramian, *Applied Mathematics & Information Sciences* 367 (2009).
- [63] A. N. Khorramian and S. A. Tehrani, *Phys. Rev. D* **78**, 074019 (2008).
- [64] A. N. Khorramian, H. Khanpour, and S. Atashbar Tehrani, *Proc. Sci., EPS-HEP2009* (2009) 393.
- [65] H. Khanpour, A. N. Khorramian, S. Atashbar Tehrani, and A. Mirjalili, *Acta Phys. Pol. B* **40**, 2971 (2009).
- [66] A. N. Khorramian, H. Khanpour, and S. A. Tehrani, *Phys. Rev. D* **81**, 014013 (2010).
- [67] E. Leader, A. V. Sidorov, and D. B. Stamenov, *Int. J. Mod. Phys. A* **13**, 5573 (1998).
- [68] Ali. N. Khorramian, S. Atashbar Tehrani, F. Olness, S. Taheri Monfred, and F. Arbabifar, *Nucl. Phys. B, Proc. Suppl.* **207**, 65 (2010); F. Arbabifar, Ali. N. Khorramian, S. Atashbar Tehrani, and A. Najafgholi, *Proceedings of the Conference in Honor of Murray Gell-Mann's 80th Birthday* (World Scientific, Singapore, 2010), pp. 503–510.
- [69] A. Mirjalili, A. N. Khorramian, S. Atashbar Tehrani, and H. Mahdizadeh Saffar, *Acta Phys. Pol. B* **40**, 2965 (2009).
- [70] A. N. Khorramian and S. Atashbar Tehrani, arXiv:0712.2373.
- [71] A. N. Khorramian and S. Atashbar Tehrani, *AIP Conf. Proc.* **915**, 420 (2007).
- [72] A. Mirjalili, A. N. Khorramian, and S. Atashbar-Tehrani, *Nucl. Phys. B, Proc. Suppl.* **164**, 38 (2007).
- [73] A. Mirjalili, S. Atashbar Tehrani, and A. N. Khorramian, *Int. J. Mod. Phys. A* **21**, 4599 (2006).
- [74] C. Amsler *et al.* (Particle Data Group), *Phys. Lett. B* **667**, 1 (2008).
- [75] A. Vogt, *Comput. Phys. Commun.* **170**, 65 (2005).
- [76] D. Stump *et al.*, *Phys. Rev. D* **65**, 014012 (2001).
- [77] M. Lacombe, B. Loiseau, R. Vinh Mau, J. Cote, P. Pires, and R. de Tourreil, *Phys. Lett. B* **101**, 139 (1981); W. W. Buck and F. Gross, *Phys. Rev. D* **20**, 2361 (1979); M. J. Zuilhof and J. A. Tjon, *Phys. Rev. C* **22**, 2369 (1980); R. Machleidt, K. Holinde, and C. Elster, *Phys. Rep.* **149**, 1 (1987); A. Y. Umnikov, L. P. Kaptari, K. Y. Kazakov, and F. C. Khanna, arXiv:hep-ph/9410241.
- [78] S. Wandzura and F. Wilczek, *Phys. Lett. B* **72**, 195 (1977).
- [79] A. Piccione and G. Ridolfi, *Nucl. Phys.* **B513**, 301 (1998).
- [80] J. Blümlein, H. Böttcher, and A. Guffanti, *Nucl. Phys.* **B774**, 182 (2007); *Nucl. Phys. B, Proc. Suppl.* **135**, 152 (2004).
- [81] S. Alekhin, J. Blümlein, S. Klein, and S. Moch, *Phys. Rev. D* **81**, 014032 (2010).
- [82] M. Glück, E. Reya, and C. Schuck, *Nucl. Phys.* **B754**, 178 (2006); P. Jimenez-Delgado and E. Reya, *Phys. Rev. D* **79**, 074023 (2009).
- [83] A. D. Martin, W. J. Stirling, R. S. Thorne, and G. Watt, *Eur. Phys. J. C* **64**, 653 (2009).
- [84] S. I. Alekhin, J. Blümlein, and S.-O. Moch, Report No. DESY 10-065 (unpublished).
- [85] V. Radescu *et al.* (H1 and ZEUS Collaboration) Combined H1 and ZEUS Fits Using Low Energy Data, talk, DIS 2010, Florence (2010); F. D. Aaron *et al.* (H1 Collaboration and ZEUS Collaboration), *J. High Energy Phys.* **01** (2010) 109.
- [86] S. Bethke, *Eur. Phys. J. C* **64**, 689 (2009).
- [87] M. M. Yazdanpanah, A. Mirjalili, S. Atashbar Tehrani, and F. Taghavi-Shahri, *Nucl. Phys.* **A831**, 243 (2009).
- [88] F. R. P. Bissey, V. A. Guzey, M. Strikman, and A. W. Thomas, *Phys. Rev. C* **65**, 064317 (2002).
- [89] F. R. P. Bissey, A. W. Thomas, and I. R. Afan, *Phys. Rev. C* **64**, 024004 (2001).
- [90] I. R. Afan *et al.*, *Phys. Rev. C* **68**, 035201 (2003).
- [91] J. D. Bjorken, *Phys. Rev.* **148**, 1467 (1966).
- [92] B. Budick, J. S. Chen, and H. Lin, *Phys. Rev. Lett.* **67**, 2630 (1991).